Single-photon multiple ionization of argon in the K-edge region

Dane V. Morgan and Roger J. Bartlett
Los Alamos National Laboratory, Los Alamos, New Mexico 87545

M. Sagurton
Los Alamos National Laboratory/SFA, National Synchrotron Light Source, Bldg. 725-X8, Brookhaven National Laboratory, Upton, New York 11973

(Received 23 September 1994)

The individual charge state and total ion yields resulting from the photoionization of argon gas have been measured as a function of photon energy through the K edge using synchrotron radiation and time-of-flight spectroscopy. We have formulated a model for the mean ion charge $\bar{q}(h\nu)$ observed at nominal photon energy $h\nu$, and have determined the mean ion charge $\bar{q}$ resulting from the decay of the atom following $[1s]4p$, $[1s]5p$, and $[1s]\varepsilon p$ photoabsorption. We have also characterized the energy-dependent photoelectron recapture probability due to postcollision interaction. In contrast with the recent analysis by Doppelfeld *et al.* [J. Phys. B **26**, 445 (1993)], we find that the gradual increase in $\bar{q}(h\nu)$ that begins approximately 20 eV below the argon K edge can be attributed to lifetime energy broadening of the K-hole state and the finite energy width of the x-ray source.

PACS number(s): 32.80.Fb, 32.80.Rm

When an inner-shell vacancy is produced in a heavy atom by x-ray photoabsorption, the excited atom can decay in a complex variety of ways, usually involving a cascade of radiative and/or nonradiative Auger or Coster-Kronig (CK) transitions. Contributing to the complexity, nonradiative transitions can sometimes be accompanied by shake-up or shake-off of one or more of the remaining electrons. In addition, an electron excited to a low-lying continuum state can be recaptured in conjunction with a subsequent Auger decay in the so-called postcollision interaction (PCI) [1–5]. For example, following a $[ls]\varepsilon p$ excitation in argon (where [ ] denotes a hole, and ε represents the energy above the continuum threshold), initial Auger decay of the K hole by $[ls]\rightarrow[2s^2]$, $[ls]\rightarrow[2s2p]$, or $[ls]\rightarrow[2p^2]$ results in a maximum ion charge state from subsequent Auger decay (in the absence of associated shake-up or shake-off) of $+6$, $+5$, or $+4$, respectively [6].

The mean final ion charge $\bar{q}$ resulting from photoabsorption in a given inner shell can be considered a function of the photoabsorption final state. Its value is determined by the probability associated with each of the pathways by which the atom can decay. Thus, when photoabsorption is not accompanied by shake-up or shake-off, the excited states for K-shell excitation are $[ls]np$ or $[ls]\varepsilon p$, and each is associated with a particular mean final ion charge $\bar{q}_{np}$ or $\bar{q}_{\varepsilon p}$. For continuum excitations just above threshold, $\bar{q}_{\varepsilon p}$ is expected to increase with ε, since the probability that the εp electron will be recaptured through PCI decreases. Within a few eV of threshold, $\bar{q}_{\varepsilon p}$ approaches its asymptotic value as the probability of recapture approaches zero. In general, there is an increased probability that the ion will retain an "extra" electron near the K edge relative to the case of $[ls]\varepsilon p$ excitations in the $\varepsilon\rightarrow\infty$ limit; and it is furthermore expected that $\bar{q}_{np}$ will tend to increase with increasing ε_{np} (the energy of the np state), because shake-off of the np electron will be less likely if the electron is more tightly bound.

Argon K-shell ionization was first observed with time-of-flight (TOF) ion-state spectroscopy by Carlson and Krause [7], who used a filtered titanium $K\alpha$ x-ray source at a fixed energy of approximately 4.5 keV. The development of intense monochromatic synchrotron radiation sources has made possible the measurement of individual ion charge state yields as a function of photon energy. TOF experiments at the argon K edge have been performed for ions formed in coincidence with K-LL Auger electrons [5], and recently, for ion states formed in coincidence with zero-kinetic energy electrons [8]. These coincidence experiments typically use an electron of well-defined energy as the start pulse for TOF timing. In contrast, our TOF system (described below) extracts ions from an interaction region with a pulsed electric field which also serves as the start pulse, and the ion collection probability varies only slightly for most ion charge states. This technique has also been utilized by Ueda *et al.* [4] for TOF studies of argon in the K-edge region.

Doppelfeld *et al.* [1] have recently performed a TOF ion charge state yield experiment for argon K-edge photoionization, in which detected electrons without energy discrimination were used as the timing start pulse. The results of this experiment showed a gradual increase in the measured mean charge $\bar{q}(h\nu)$ from photoionization, beginning many K-hole energy widths below the argon $[ls]4p$ resonance excitation, but the explanation for this observation was left as an open question. Recently, Amusia [6] offered an explanation for this increase in $\bar{q}(h\nu)$ in terms of virtual excitation of the $[ls]\varepsilon p$ state. However, Amusia's semi-quantitative analysis neglects the effects of $[ls]np$ excitations and the energy bandwidth of the photon source.

Interestingly, a very similar phenomenon was observed by Holland *et al.* [9] in their observations of the double

photoionization cross section of argon gas 20 to 30 eV below the $L_{2,3}$ edge. This problem was addressed in a many-body perturbation theory (MBPT) calculation by Pan and Kelly [10] that included the effects of virtual excitation of the $L_{2,3}$ hole states below the $L_{2,3}$ edge. This analysis yielded a result qualitatively similar to the experimental result, but the increase in the double ionization cross section below the $L_{2,3}$ edge was considerably smaller than the increase reported by Holland *et al.*

We have measured the distribution of ion charge states produced by the photoionization of argon as a function of photon energy through the K-edge region. Results are presented for the $h\nu$-dependent total ion yield $I(h\nu)$ and mean ion charge $\bar{q}(h\nu)$. We develop quantitative models for $I(h\nu)$ and $\bar{q}(h\nu)$ that incorporate the effects of natural line broadening and the finite-energy width of the photon source. We are thus able to extract the mean ion charge $\bar{q}_{np}$ and $\bar{q}_{\varepsilon p}$, resulting from the decay of the atom following $[ls]np$ and $[ls]\varepsilon p$ excitations, respectively. The effects of PCI on $\bar{q}_{\varepsilon p}$ are also characterized.

The experiments were performed on beamline X8A at the National Synchrotron Light Source. Light from the storage ring was incident at 10 mrad on a Ni-coated, bent cylinder, double focusing mirror, and monochromatized with a Si(111) crystal pair in the $(1,-1)$ nondispersive configuration with a Si(111) crystal pair in the $(1,-1)$ nondispersive configuration. Harmonic light was effectively eliminated by the reflectivity cutoff of the focusing mirror at 5.9 keV. A 0.5-μm nickel filter downstream from the monochromator was used to eliminate broadband, specularly reflected, low-energy radiation from the beam. Magnets were placed upstream and downstream from the TOF chamber to prevent stray electrons from reaching the TOF interaction region.

The experimental setup is shown in Fig. 1. The beam was incident on a gas target created in the interaction region of the TOF spectrometer by an effusive gas jet. The gas sample chamber was maintained at 1.0×10^{-6} torr partial pressure of argon, after evacuating the system to a base pressure of approximately 10^{-9} torr. The TOF spectrometer was of the Wiley-McLaren type [11] and has been described previously [12]. TOF start pulses were generated by a PC-controlled time-to-digital converter (TDC) board [13]. The TDC board had a time resolution of 2.5 nsec, and was capable of recording multiple events in a single pulse repetition time (PRT) interval. A constant PRT of 15 μsec was maintained. Each start pulse triggered two high voltage pulsers for generation of an extraction field of $\approx$23 V/mm and an acceleration field of $\approx$80 V/mm. After leaving the extraction and acceleration regions, the ions passed through a field-free region, followed by a post acceleration potential of -5.4 keV prior to being detected by dual, chevron microchannel plates (MCP's). The detected ion signal was amplified, filtered, and returned to the TDC board as the timing stop pulse. To total ion flight time in the TOF spectrometer was approximately proportional to the square root of the mass-to-charge ratio, and thus different ion charge states were resolved. For each photon energy, the TOF spectrum was collected and converted into a data file by the computer.

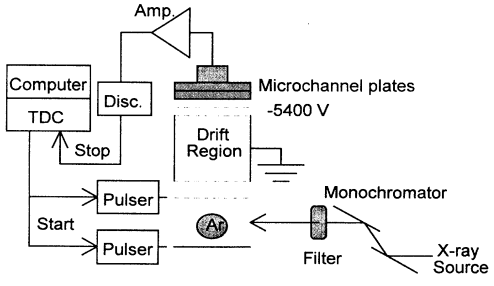

FIG. 1. Experimental setup.

If an ion created in the interaction region has a sufficiently large velocity component perpendicular to the TOF axis, its transverse drift may prevent it from reaching the MCP detector. This effect can reduce the overall collection efficiency of the TOF spectrometer, which thus depends both on the thermal motion of the ions and the ion recoil associated with electron emission during photoabsorption or Auger decay. In general, the collection efficiency tends to be slightly larger for higher charge states since the flight time is shorter. We have developed a Monte Carlo computer simulation of the TOF spectrometer in order to quantitatively determine the collection efficiency for each ion charge state, taking into consideration both the ion recoil velocity and the Maxwell-Boltzmann thermal velocity distribution. The transitions that were found to impart sufficient ion recoil so as to significantly reduce the collection efficiency were photoabsorption of the $\approx$3.2-keV photon by an M- or L-shell electron, and Auger decay of a K hole. The corresponding recoil energies are approximately 0.043, 0.040, and 0.036 eV, respectively. In practice, these differences are not significant. The recoil from Auger decay of an L hole is small compared with the thermal energy and can be neglected. The ion charge states Ar^{3+} through Ar^{8+} produced following K-shell photoabsorption are assumed to involve K-hole Auger decay, since the relative probability for pathways involving K-L fluorescence is small [1,4]. However, production of Ar^{+} and Ar^{2+} following K-shell photoabsorption results primarily from K-M and K-L fluorescence [1,4]. Our Monte Carlo simulations showed that the collection efficiencies for the different charge states are nearly equal, with the exception of Ar^{+} and Ar^{2+} ions formed following K-shell radiative emission, for which the efficiencies are $\approx$20% higher due to negligible ion recoil.

TOF spectra were recorded for photon energies in increments of 0.1 eV through the argon K-edge region. A typical TOF spectrum ($h\nu=3203.6$ eV) is shown in Fig. 2. The areas of the eight ion charge state peaks were calculated, then corrected for the acquisition time (typically 300 sec) and collection efficiencies to obtain the yields of the individual ion charge states and the total ion yield $I(h\nu)$. The mean ionic charge from photoionization $\bar{q}(h\nu)$ was determined from the fractional yields of the ion charge states. Beam current variations were normalized out using the signal from an aluminum x-ray diode

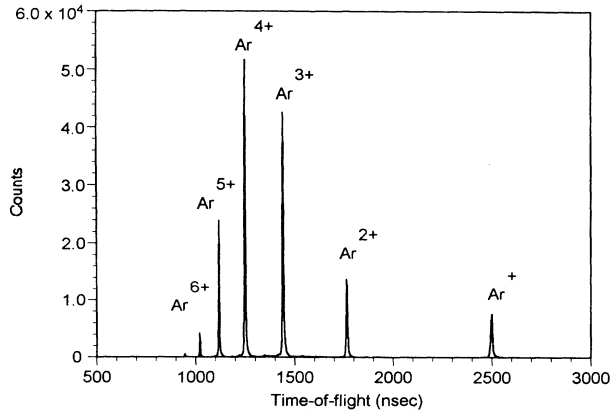

FIG. 2. Argon TOF spectrum at 3203.6 eV. The acquisition time for this spectrum was 300 sec.

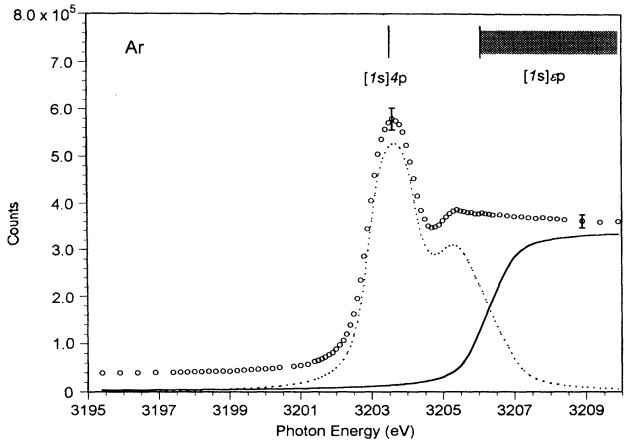

FIG. 3. Total ion yield spectrum. The open circles represent the total ion yield data $I(h\nu)$. The dotted line represents the least-squares fit for the line-broadened total cross section for Rydberg excitations, i.e., the sum of all $\sigma_{np}(h\nu)$. The solid line is the least-squares fit for the cross section $\sigma^{\Sigma}_{[ls]}(h\nu)$ for continuum excitations.

detector mounted at the end of the beam path. The x-ray detector efficiency was essentially constant over the small energy range near the argon K edge. The monochromator energy scale was calibrated using the accepted value of 3203.5 eV for the $[ls]4p$ excitation energy [14].

The total ion yield $I(h\nu)$, shown in Fig. 3, reproduced the principal features of the argon K-edge x-ray absorption spectrum. Breinig *et al.* [14] and Parratt [15] have shown that this absorption spectrum can be represented as the sum of δ functions for the $[ls]np$ resonance excitations and a step function for the total cross section for $[ls]\varepsilon p$ continuum excitations, convoluted with appropriate functions representing the final state lifetime and the finite energy width of the x-ray source. We have used this model to determine the cross sections for $[ls]np$ and $[ls]\varepsilon p$ transitions by fitting the model spectrum to the total ion yield data as a function of photon energy in a least-squares calculation. The intrinsic absorption line shape for a $[ls]np$ or $[ls]\varepsilon p$ excitation is defined as the photon energy dependent cross section for producing the given transition with a perfectly monochromatic beam. It is represented by a Lorentzian function with full width at half maximum equal to Γ, where Γ represents the hole energy width. A pulse function (described below) of energy width a was chosen to approximate the finite photon energy distribution from the monochromator. This energy spread was caused mostly by the divergence of the photon beam and not the rocking curve of the monochromator crystals. The model line shape $\sigma_{np}(h\nu)$ describing the cross section for a $[ls]np$ excitation with nominal photon energy $h\nu$ is proportional to the convolution of the lifetime and instrumental broadening functions

$$\sigma_{np}(h\nu)\propto\int_{-\infty}^{\infty}\left[\Theta\left[h\nu-E+\frac{a}{2}\right]-\Theta\left[h\nu-E-\frac{a}{2}\right]\right]\left[1+\left[\frac{E-E_{np}}{\Gamma/2}\right]^2\right]^{-1}dE\ , \tag{1}$$

or

$$\sigma_{np}(h\nu)=A_{np}\left[\tan^{-1}\left[\frac{h\nu-E_{np}+a/2}{\Gamma/2}\right]-\tan^{-1}\left[\frac{h\nu-E_{np}-a/2}{\Gamma/2}\right]\right], \tag{2}$$

where Θ is the unit step function, $\Theta(h\nu-E+a/2)-\Theta(h\nu-E-a/2)$ is a pulse function of energy width a with a mean energy E, $E_{np}=\varepsilon_{np}-\varepsilon_{ls}$ is the excitation energy of the $[ls]np$ state, and A_{np} is a constant. The model line shape $\sigma_{\varepsilon p}(h\nu)$ has a form similar to Eq. (2) for any value of ε. Integrating over ε gives the line shape $\sigma^{\Sigma}_{[ls]}(h\nu)$ for the complete set of $[ls]$ continuum excitations

$$\sigma^{\Sigma}_{[ls]}(h\nu)\propto\int_0^{\infty}\sigma_{\varepsilon p}(h\nu)d\varepsilon\ , \tag{3}$$

or

$$\sigma^{\Sigma}_{[ls]}(h\nu)=A^{\Sigma}_{[ls]}\left[\frac{\pi a}{\Gamma}-\left[\frac{h\nu-E_0-a/2}{\Gamma/2}\right]\tan^{-1}\left[\frac{h\nu-E_0-a/2}{\Gamma/2}\right]+\left[\frac{h\nu-E_0+a/2}{\Gamma/2}\right]\tan^{-1}\left[\frac{h\nu-E_0+a/2}{\Gamma/2}\right]+\ln\left[\frac{(\Gamma/2)^2+(h\nu-E_0-a/2)^2}{(\Gamma/2)^2+(h\nu-E_0+a/2)^2}\right]^{1/2}\right], \tag{4}$$

where the $E_0 = -\varepsilon_{ls}$ is the threshold continuum excitation energy and $A^{\Sigma}{}_{[ls]}$ is a constant. We have neglected the energy dependence of the matrix element over the narrow energy range near the K edge. The values for A_{4p}, A_{5p}, and $A^{\Sigma}{}_{[ls]}$ were determined from the optimization of the least-squares fit. Established values were used for E_{4p}, E_{5p}, and E_0 from the work of Breinig *et al.* [14]. We were unable to resolve the high-lying Rydberg states $[ls]np, n \geq 6$ so these states were represented in our model by a single function of the form of Eq. (2), with independently variable parameters A_{6p}, E_{6p}, and a for optimization of the least-squares fit. The resultant K-edge absorption model function for the total ion yield data is also shown in Fig. 3. Results of the analysis gave a value for the parameter a of 1.31 eV, which approximates the photon energy bandpass of the monochromator. The value for Γ, the full width of lifetime energy broadening, was 0.69 eV, which agrees closely with the accepted value [16] of 0.68 eV. This agreement may be fortuitous, because our pulse function model is an imperfect representation of the source energy bandpass.

Our experimental result for $\bar{q}(h\nu)$, the mean ion charge as a function of photon energy, is shown is Fig. 4. Our values for $\bar{q}(h\nu)$ are approximately 15% lower than those reported by Doppelfeld *et al.* [1], although similar trends in the spectra are observed. Because Doppelfeld *et al.* used electrons, without energy discrimination, as the timing start pulse, there is an inherent bias in their system towards the detection of the more highly ionized states, which release more electrons and are therefore more likely to be detected. A crude correction may be applied to the data of Doppelfeld *et al.* by assuming that the probability for detection of a given ion charge state is proportional to the charge of that ion state. When this correction is performed, much closer agreement with our results is obtained.

Because the various $\sigma_{np}(h\nu)$, $\sigma_{\varepsilon p}(h\nu)$ as well as the σ_L and σ_M (L- and M-shell cross section) overlap, at any $h\nu$ the experimental $\bar{q}(h\nu)$ represents a weighted average of the $\bar{q}_{np}$, $\bar{q}_{\varepsilon p}$, $\bar{q}_L$, and $\bar{q}_M$. Below, we describe a procedure for extracting the $\bar{q}_{np}$ and $\bar{q}_{\varepsilon p}$. First, however, it is of interest to compare experiment with the result one obtains for $\bar{q}(h\nu)$ by letting $\bar{q}_{np}$ and $\bar{q}_{\varepsilon p}$ equal the limit of $\bar{q}_{\varepsilon p}$ as $\varepsilon \to \infty$; in effect, neglecting the increased probability that the ion will ultimately retain an "extra" electron for K-shell photoabsorption near the edge. Following Tonuma *et al.* [17], let $\sigma_i(h\nu)$, $i = K,L,M$ be the total cross section for i-shell photoabsorption for nominal photon energy $h\nu$, and let $\bar{q}_i$ be the mean final ion charge from i-shell photoabsorption in the high $h\nu$ limit. We then have

$$\bar{q}(h\nu) = \sum_{i=K,L,M} \bar{q}_i \sigma_i(h\nu) \left[\sum_{i=K,L,M} \sigma_i(h\nu) \right]^{-1} . \quad (5)$$

We shall use Eq. (5) as the basis for our model calculation of $\bar{q}(h\nu)$.

From a TOF spectrum for an excitation energy well below the K edge, we have determined the value for the mean charge for the ion states formed by L- and M-shell excitation $\bar{q}_{LM}$, to be 2.65 ± 0.06 in units of the fundamental charge e. Variations in this quantity with photon energy over the narrow energy range of this experiment are quite small and have been neglected. Subtracting the individual charge state ion yields at photon energies well below the K edge from the ion yields at a photon energy of 3215 eV, where PCI effects are negligible [1,4], we have determined the value of $\bar{q}_K$, the mean charge produced by $[ls]\varepsilon p$ excitations in the high $h\nu$ limit, to be $3.91 \pm 0.09e$. $\Sigma\sigma_i(h\nu)$ is simply the total ion yield as a function of energy $I(h\nu)$. If σ_{LM} is the (approximately constant) total ion yield well below the K edge, then $\sigma_K(h\nu)$ is the difference between $\Sigma\sigma_i(h\nu)$ and σ_{LM}.

$\bar{q}(h\nu)$ determined from Eq. (5) is compared with experimental values in Fig. 4. Both curves show a similar gradual increase for photon energies from 3180 to 3195 eV, which is significant because it implies that lifetime and instrument broadening are responsible for the increase. The large difference between the two curves in Fig. 4 for 3195 eV $< h\nu <$ 3215 eV clearly shows the reduction in $\bar{q}(h\nu)$ that results from the increased probability that the ion will retain an extra electron.

To incorporate this reduction in mean charge in the K-edge region, we must modify Eq. (5) to have the following form:

$$\bar{q}(h\nu) = \frac{\bar{q}_{LM}\sigma_{LM} + \sum_{n=4}^{\infty} \bar{q}_{np}\sigma_{np}(h\nu) + \int_0^{\infty} \bar{q}_{\varepsilon p}\sigma_{\varepsilon p}(h\nu)\, d\varepsilon}{\sum_{i=K,L,M} \sigma_i(h\nu)} . \quad (6)$$

The quantum-mechanical form for $\bar{q}_{\varepsilon p}$, which accounts for the recapture probability due to PCI following a $[ls]\varepsilon p$ excitation, has been given by Tulkki *et al.* [3] as

$$\bar{q}_{\varepsilon p} = \bar{q}_K - C[1 - \exp(-\Gamma/\varepsilon)], \quad 0 < C \leq 1 , \quad (7)$$

where C is a constant. However, we have chosen to represent $\bar{q}_{\varepsilon p}(E)$ with the simpler linear approximation given by Ueda *et al.* [4],

$$\bar{q}_{\varepsilon p} = \begin{cases} \bar{q}_K + \beta(\varepsilon - \varepsilon_c), & 0 \leq \varepsilon \leq \varepsilon_c \\ \bar{q}_K, & \varepsilon > \varepsilon_c \end{cases} \quad (8)$$

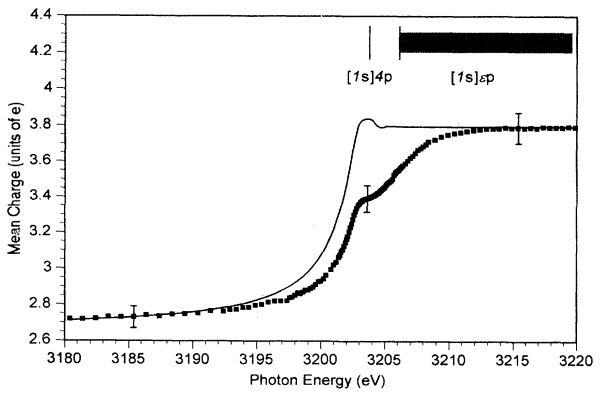

FIG. 4. Mean charge $\bar{q}$ as a function of photon energy. The closed boxes are the experimental values for $\bar{q}(h\nu)$. The solid line represents the model values for $\bar{q}(h\nu)$ obtained from Eq. (5).

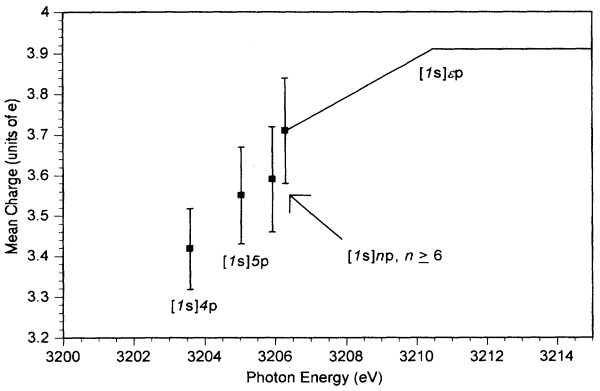

FIG. 5. Values for the mean ion charge $\bar{q}_{np}$ and $\bar{q}_{\varepsilon p}$ resulting from the decay of $[ls]np$ and $[ls]\varepsilon p$ excitations.

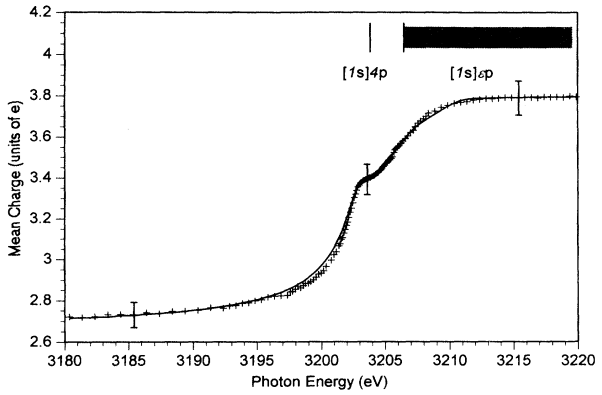

FIG. 6. Experimental and model calculation values for $\bar{q}(h\nu)$. Plus signs are the experimental values for the mean ion charge $\bar{q}(h\nu)$. The solid line represents the model values for $\bar{q}(h\nu)$ obtained from Eq. (6) using the values for $\bar{q}_{np}$ and $\bar{q}_{\varepsilon p}$ shown in Fig. 5.

where ε_c and β are constants in order to simplify the integration in Eq. (6). ε_c represents the energy cutoff above which PCI effects do not occur.

We have performed a least-squares calculation to determine the parameters $\bar{q}_{np}$, ε_c, and β that minimize the difference between Eq. (6) and the experimental $\bar{q}(h\nu)$. Figure 5 shows the results for $\bar{q}_{\varepsilon p}$ and $\bar{q}_{np}$ and illustrates the reduction in the mean ion charge with decreasing energy (below ε_c). The values determined for the parameters in Eq. (6) are $\bar{q}_{4p}=3.42\pm0.10e$, $\bar{q}_{5p}=3.55\pm0.15e$, $\beta=0.053\pm0.004e/\text{eV}$, and $\varepsilon_c=3.85\pm0.18$ eV. The difference between $\bar{q}_{4p}$ and $\bar{q}_K$ is $0.49\pm0.02e$, which agrees with the value determined by Doppelfeld [18] of $0.49\pm0.03e$. Figure 6 shows the comparison between our experimental values for $\bar{q}(h\nu)$ and Eq. (6). The close agreement obtained throughout the energy range establishes that the same lifetime or instrumental broadening accounts both for the width of the edge rise and the gradual increase in $\bar{q}(h\nu)$ for $h\nu$ between 3180 and 3195 eV. This analysis also suggests a possible explanation for the discrepancy between the experimental and theoretical results for the double ionization cross section below the argon $L_{2,3}$ edge. The energy bandpass of the photon source reported by Holland *et al.* [9] was approximately 9 eV at the photon energies in question. This is approximately two orders of magnitude larger than the L-shell natural energy width and was not included in the Pan and Kelly calculations [10]. We suggest that the inclusion of the photon energy bandpass in the calculation would reduce or eliminate this discrepancy.

In conclusion, we have measured the total ion yield and mean ion charge resulting from photoionization of argon through the K edge. We have determined the mean charge resulting from the decay of the atom following $[ls]4p$, $[ls]5p$, and $[ls]\varepsilon p$ photoabsorption. Also, we have verified the gradual increase in $\bar{q}$ beginning approximately 20 eV below the argon K edge observed by Doppelfeld *et al.* and have shown by quantitative analysis that this structure is entirely attributable to the lifetime broadening of the K-hole states and the finite energy width of the source.

This material is based on work supported by the U.S. Department of Energy through Los Alamos National Laboratory.

[1] J. Doppelfeld, N. Anders, B. Esser, F. von Busch, H. Scherer, and S. Zinz, J. Phys. B. **26**, 445 (1993).
[2] W. Eberhardt, S. Bernstorff, H. W. Jochims, S. B. Whitfield, and B. Crasemann, Phys. Rev. A **38**, 3808 (1988).
[3] J. Tulkki, T. Åberg, S. B. Whitfield, and B. Crasemann, Phys. Rev. A **41**, 181 (1990).
[4] K. Ueda, E. Shigemasa, Y. Sato, A. Yagishita, M. Ukai, H. Maezawa, T. Hayaishi, and T. Sasaki, J. Phys. B **24**, 605 (1991).
[5] J. C. Levin, C. Biedermann, N. Keller, L. Liljeby, C.-S. O, R. T. Short, I. A. Sellin, and D. W. Lindle, Phys. Rev. Lett. **65**, 988 (1990).
[6] M. Ya. Amusia, Phys. Lett. A **183**, 201 (1993).
[7] T. A. Carlson and M. O. Krause, Phys. Rev. **137**, A1665 (1965).
[8] T. Hayaishi, E. Murakami, Y. Morioka, E. Shigemasa, A. Yagishita, and F. Koike, J. Phys. B **27**, L115 (1994).
[9] D. M. P. Holland, K. Codling, J. B. West, and G. V. Marr, J. Phys. B **12**, 2465 (1979).
[10] C. Pan and H. P. Kelly, Phys. Rev. A **39**, 6232 (1989).
[11] W. C. Wiley and I. H. McLaren, Rev. Sci. Instrum. **26**, 1150 (1955).
[12] R. J. Bartlett, P. J. Walsh, Z. X. He, Y. Chung, E-M. Lee, and J. A. R. Samson, Phys. Rev. A **46**, 5574 (1992).
[13] SI Diamond, 2435 North Blvd., Houston, TX 77098.

[14] M. Breinig, M. H. Chen, G. E. Ice, R. Parente, B. Crasemann, and G. S. Brown, Phys. Rev. A **22**, 520 (1980).
[15] L. G. Parratt, Phys. Rev. **56**, 295 (1939).
[16] M. O. Krause and J. H. Oliver, J. Phys. Chem. Ref. Data **8**, 329 (1979).
[17] T. Tonuma, A. Yagishita, H. Shibata, T. Koizumi, T. Matsuo, K. Shima, T. Mukoyama, and H. Tawara, J. Phys. B **20**, L31 (1987).
[18] J. Doppelfeld, Diploma thesis, Bonn University, 1991 (unpublished).